A 4DVAR-aware method of decomposing geophysical model fields into eddy and background components

Robert Keenan Forney[1]
[1] Naval Research Laboratory, Stennis Space Center, MS 39529
Contact: Dr. Robert Keenan Forney (robert.k.forney.civ@us.navy.mil)

ABSTRACT

Chaotic amplification of errors arises in four-dimensional variational data assimilation (4DVAR) due to inherent nonlinearity of the physical system being observed and modelled. The ocean state can be thought of as decomposing into a nonlinear eddy field and a linear background field. Here, a new method is investigated to define the eddy field in terms of goals for the balance, conservation, and error growth potential of the background field that results from subtracting the eddy field from the ocean state. The eddy field is learned by a U-net given only sea surface height (SSH) for 16 ensemble members (4 held for validation) of weekly-averaged six-year (2020-2025) ~30km ECCO runs, so the operators are calibrated using ECCO 1deg monthly reanalysis spanning 1999-01 to 2019-12 (28 years) then applied to learning on sixteen of twenty free run ensemble of SSH (four held out for validation). There are significant differences between the otherwise similar learned eddy field and traditional climatological and ensemble eddy fields that should be investigated further that may point to improvements in the implementation or insights about how oceanographic features correlate spatiotemporally with features that impact 4DVAR performance. In terms of how suitable the background is for 4DVAR, the learned eddy field outperforms climatology and ensemble in 11/13 tiles, underperforming in the polar tiles. This pattern persisted when the model was applied to higher-resolution snapshots.

4DVAR MOTIVATION

$$e^* = \arg\min_e \left(\|e\|_W^2 + \alpha\|\nabla e\|_W^2\right) \quad \text{s.t.} \quad b = x - e, \quad Ce = 0, \quad B(b) \approx 0, \quad \gamma_T(b) \le \gamma^*$$

$$\mathcal{L}(e) = \|e\|_W^2 + \alpha\|\nabla e\|_W^2 + \lambda_C\|Ce\|^2 + \lambda_B\|B(x-e)\|^2 + \lambda_\gamma\,\mathrm{relu}\big(\gamma_T(x-e) - \gamma^*\big)^2 + \lambda_{\mathrm{wave}}\mathcal{L}_{\mathrm{wave}}(e) + \lambda_{\mathrm{floor}}\mathcal{L}_{\mathrm{floor}}(e)$$

Component	Mathematical Definition	Theoretical & Physical Role
$b = x - e$	Exact Identity	Background falls out by subtraction; exact reconstruction by construction.
$\|e\|_W^2$	$\sum_{\mathrm{pos}} e^2 W$	Minimum-norm regularization (Occam's razor). Area weight $W = \frac{\mathrm{RAC}\cdot\mathrm{maskC}}{\sum(\mathrm{RAC}\cdot\mathrm{maskC})}$.
$\alpha\|\nabla e\|_W^2$	$\alpha\sum_{\mathrm{pos}}\|\nabla e\|^2 W$	H^1 Tikhonov regularization. Suppresses unphysical grid-scale noise ($\alpha = 3\times10^9$).
$Ce = 0$	Multi-scale Block Averaging	Integral mass/volume conservation. Eddies redistribute fluid without net inventory drift.
$B(b) \approx 0$	$\mathrm{Ro}(b) = \frac{g}{f^2}\nabla^2 b$	Kinematic Rossby balance. Background vorticity must remain within the geostrophic regime ($\mathrm{Ro} \ll 1$).
$\gamma_T(b) \le \gamma^*$	Finite-Time Growth Operator	Caps perturbation growth rates to prevent tangent-linear instability in 4D-Var windows.

$$L_d = \frac{NH}{\pi f}, \qquad T_d \sim \frac{1}{\sigma}$$

$$w_k(s_k, L_d) = \frac{\left(\frac{s_k}{L_d}\right)^p}{1 + \left(\frac{s_k}{L_d}\right)^p}$$

$$\mathcal{L}_{\mathrm{wave}}(e) = \sum_{k=1}^{K} w_k\|\mathrm{detail}_k(e)\|_W^2$$

$$u_g = -\frac{g}{f}\frac{\partial b}{\partial y}, \quad v_g = \frac{g}{f}\frac{\partial b}{\partial x}, \quad \zeta_g = \frac{\partial v_g}{\partial x} - \frac{\partial u_g}{\partial y} = \frac{g}{f}\nabla^2 b, \quad Ro(b) = \frac{\zeta_g}{f} = \frac{g}{f^2}\nabla^2 b$$

Figure 1. The objective is to learn an (area-weighted) eddy field e that is as small and smooth as possible then compute the background b from the identity b = x – e where x is the model state. C enforces the constraint that the eddy field doesn't create or destroy water/heat/salt by forcing the area-weighted integral of e to vanish across all scales. Because of the broad scope of validation required to apply a balance operator B learned in a different model/regime then apply to only 2D fields, B(b) is treated instead as Ro(b) in the loss function. The error growth is informed by the Rossby deformation radius L_d and eddy turnover / instability growth timescale., such that the timescale for how quickly errors should grow is grounded in f and stratification N.

LEARNED EDDY, BACKGROUND FIELD COMPARISON WITH CLIMATOLOGY AND ENSEMBLE

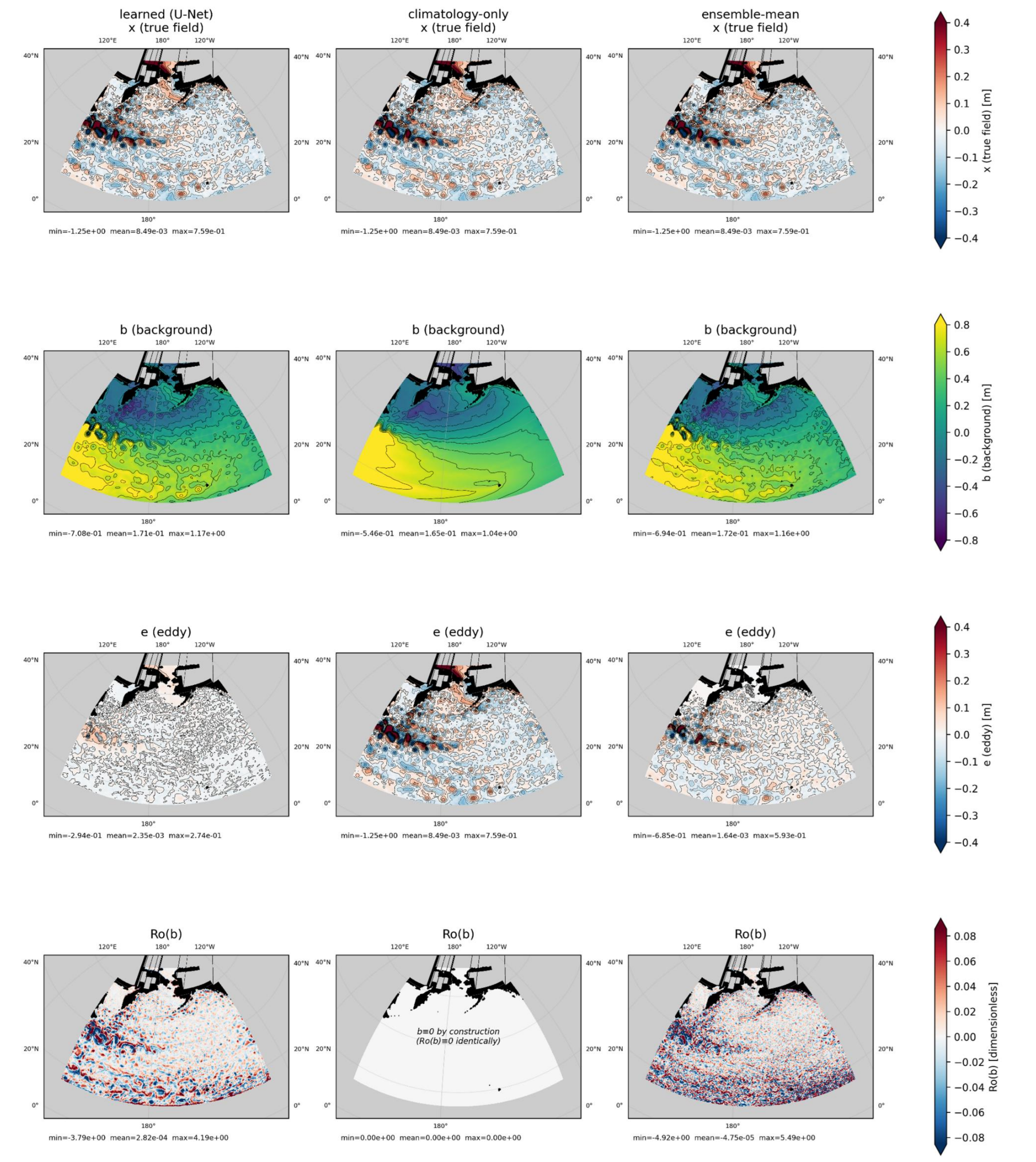

Figure 3. The original model state x (first row) is decomposed into a background (second row) and eddy field (third row), and the Rossby number of the resulting background is computed (fourth row). The learned fields (left column) have a similar level of topological complexity to the ensemble fields (right column); the climatology-based fields (center column) are exceptionally smooth in the background and have the most intense features in the eddy field. These intense features tend to amplify during 4DVAR due to their nonlinearity, while the background is too flat, making it difficult to apply reasonable increments. The learned eddy field is much smaller and smoother but shares much of the same features as ensemble. The Rossby number of the learned background is smaller (not zero like the climatology).

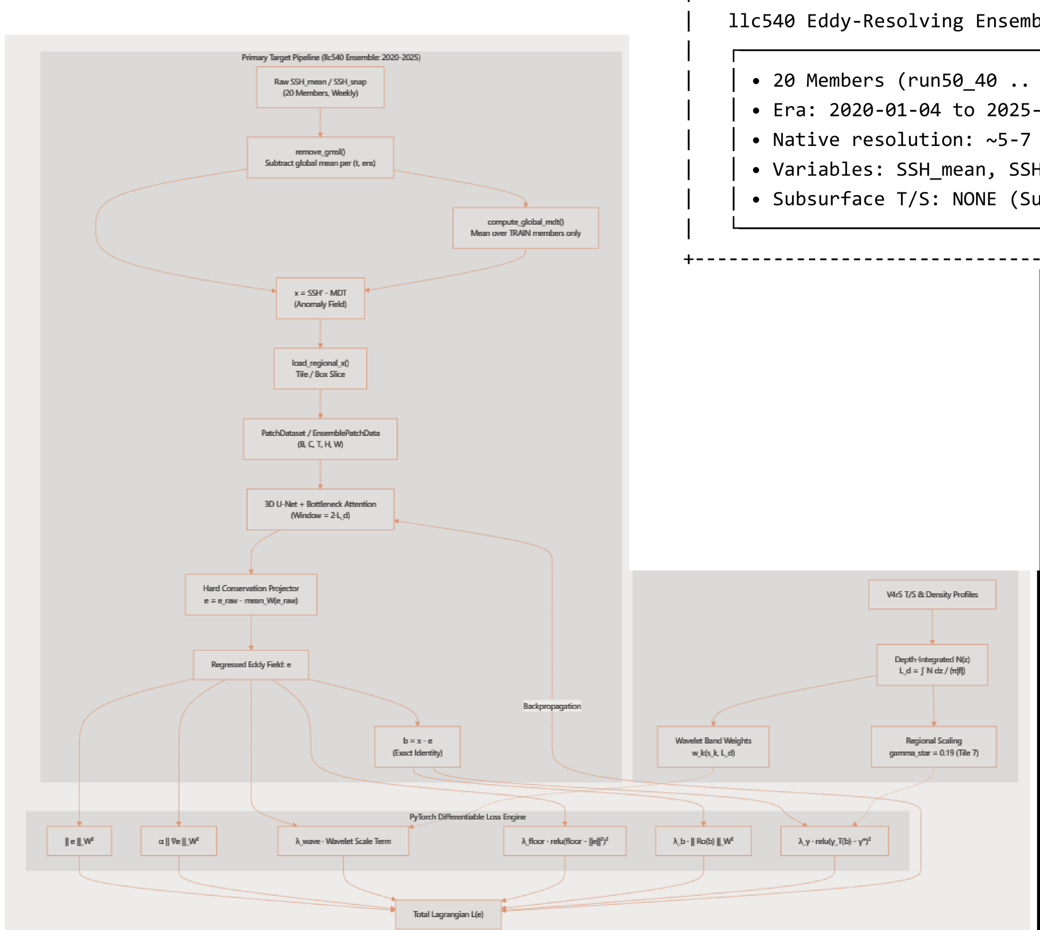

```
ECCO Data Products Architecture

llc540 Eddy-Resolving Ensemble (Primary Target)
 • 20 Members (run50_40 .. run50_59)
 • Era: 2020-01-04 to 2025-12-28 (Weekly)
 • Native resolution: ~5-7 km (540x540/tile)
 • Variables: SSH_mean, SSH_snap, OBP_mean
 • Subsurface T/S: NONE (Surface only)

llc90 V4r5 Adjoint State Estimate
 • Deterministic Reanalysis
 • Era: 1992-01 to 2019-12 (Monthly)
 • Native resolution: ~30-100 km
 • Variables: 3D T/S, Velocities, N²
 • Role: Offline Physics Calibration
```

Figure 2. The model architecture. When the learned model incorporates no scale information, e focuses on the large-scale signal, which minimizes magnitude and roughness without preserving the eddy structure associated with nonlinearity. To mitigate this, e is evaluated in a wavelet-style decomposition so that the objective function can treat each scale band separately. Weight is scaled according to the local L_d such that energy is weighted more heavily below L_d without hard-zeroing the other bands. The scaling factor lambda_wave is calibrated based on the full physics model run. Further, attention is applied to the U-net within frequency bands so that background variability should be able to draw upon large-scale context while e is mostly locally coherent. Local attention is also applied over an area that scales with the local L_d.

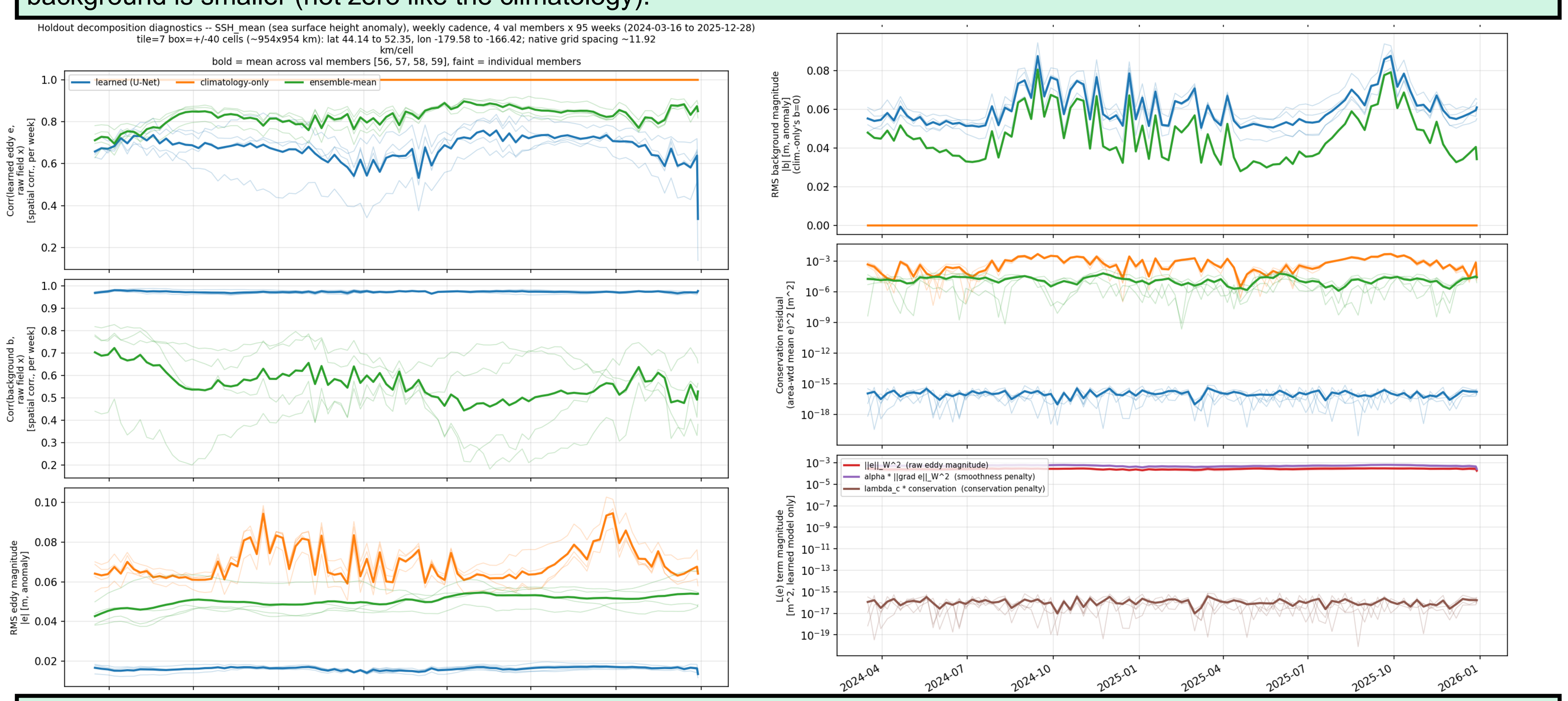

Figure 4. Validation. The success of this approach is evaluated based on whether the learned e achieves a lower L(e) than climatology's e=x or ensemble mean's e=x-mean_ens(x) on the same held-out data. If it is lower that just means gradient descent worked, so we also check how the model's e performs when evaluated on tiles it never saw at a resolution it also never saw. The learned e outperforms on 11 of 13 tiles, which generalized to unaveraged snapshots that were not part of the training data (it was trained on weekly averaged data). The contributions to L(e) are disaggregated above.

DISCUSSION

4DVAR on an eddy-resolving model can lead to unbounded growth of singular values and model failure, so it would be desirable to disaggregate the nonlinear eddy field from the background, do 4DVAR on the background, and restore the eddy field. These results focused on how to construct the suitable background and leave the details of implementation in 4DVAR to future work. The background sits on a smooth balanced manifold by construction—the fact that it outperforms climatology and ensemble means is unremarkable since the gradient descent optimization practically guarantees this result.

More remarkable is that this feature 1) extrapolates beyond the training tile to other tiles; 2) is robust across model runs and time periods that were not in the training; 3) continues to be the case when applied to higher-resolution snapshots instead of the training weekly mean; and 4) results in an eddy field that, while relatively small, aligns with features stereotypically associated with nonlinearity such as closed Okubo-Weiss contours even when the balance operator is a simple smoothness constraint (vs. Rossby number dependent in the main results). This suggests that the eddy field used to calculate the background is physically meaningful even though the objective used to calculate e is defined by desirable characteristics for 4DVAR, not kinematics. Detailed examination of how the eddy field aligns with physical phenomena of interest like fronts and eddies would be a useful future step in evaluating the usefulness of this decomposition.

The main test will be to attempt this procedure of 4DVAR on the background field before restoring eddies in an operational setup to see how it impacts stability and accuracy of the results at eddy-resolving resolutions. This would at least establish the practical value of the results; a machine-learned background field lacks some of the conceptual clarity that climatology and ensemble mean have and needs to be evaluated not just based on whether it satisfied its objective and showed generalizability but in terms of whether its solution is unique and has a useful physical interpretation. Considering the small amplitude of the learned eddy field, it represents something smaller than the deviation from typical ocean conditions or the spread of possible states that also aligns well with the most nonlinear features. A more detailed evaluation is beyond the scope of this eight-week project but would benefit from more evaluation of the field decomposition and practical results in a 4DVAR operational setup.

References:

Bannister, R. N. (2008). A review of operational methods of resolving and representing forecast error covariance in the ocean. Quarterly Journal of the Royal Meteorological Society, 134(637), 1971–1996.

Bannister, R. N. (2008). A review of forecast error covariance statistics in atmospheric variational data assimilation. I: Characteristics and methods of estimation. Quarterly Journal of the Royal Meteorological Society, 134(637), 1951–1970.

Cooper, M., & Haines, K. (1996). Altimetric assimilation with water property conservation. Journal of Geophysical Research: Oceans, 101(C1), 1059–1077.

Lorenc, A. C. (2003). The potential of the ensemble Kalman filter for NWP—a comparison with 4D-Var. Quarterly Journal of the Royal Meteorological Society, 129(595), 3183–3203.

Parrish, D. F., & Derber, J. C. (1992). The National Meteorological Center's spectral statistical-interpolation analysis system. Monthly Weather Review, 120(8), 1747–1763.

Weaver, A. T., & Courtier, P. (2001). Variational assimilation of ocean data in a comprehensive operational system. Quarterly Journal of the Royal Meteorological Society, 127(575), 1815–1846.

Weaver, A. T., Deltel, C., Machu, E., Ricci, S., & Daget, N. (2005). A multivariate balance operator for ocean data assimilation. Quarterly Journal of the Royal Meteorological Society, 131(613), 3605–3625.

Chelton, D. B., deSzoeke, R. A., Schlax, M. G., El Naggar, K., & Siwertz, N. (1998). Geographical variability of the first baroclinic Rossby radius of deformation. Journal of Physical Oceanography, 28(3), 433–460.

Chelton, D. B., Schlax, M. G., & Samelson, R. M. (2011). Global observations of nonlinear mesoscale eddies. Progress in Oceanography, 91(2), 167–216.

Eady, E. T. (1949). Long waves and cyclone waves. Tellus, 1(3), 33–52.

Isern-Fontanet, J., García-Ladona, E., & Font, J. (2003). Identification of marine eddies from altimetric data. Journal of Atmospheric and Oceanic Technology, 20(5), 772–778.

Piecuch, C. G. (2017). A note on practical evaluation of budgets in ECCO Version 4 Release 3 (Technical Report). ECCO Consortium.

Wunsch, C., & Heimbach, P. (2007). Practical global oceanic state estimation. Physica D: Nonlinear Phenomena, 230(1–2), 197–208.

Wunsch, C., & Heimbach, P. (2013). Dynamically and kinematically consistent global ocean circulation and properties. In G. Siedler, S. M. Griffies, J. Gould, & J. A. Church (Eds.), Ocean Circulation and Climate: A 21st Century Perspective (Vol. 103, pp. 553–579). Academic Press.

Odena, A., Dumoulin, V., & Olah, C. (2016). Deconvolution and checkerboard artifacts. Distill, 1(10), e3. https://doi.org/10.23915/distill.00003

Pan, S. J., & Yang, Q. (2010). A survey on transfer learning. IEEE Transactions on Knowledge and Data Engineering, 22(10), 1345–1359.

Acknowledgements: Great thanks to Ou Wang, Ian Fenty, and Matthew Mazloff for the inspiration, support, model results, and constructive feedback, as well as Jinbo Wang and Georgy Manucharyan whose AI4Ocean Workshop made our discussion possible.

This work was funded by the U.S. Naval Research Laboratory Karles Fellowship program.